Arabian Journal of Chemistry (2013) 6, 379–388

King Saud University

Arabian Journal of Chemistry

www.ksu.edu.sa
www.sciencedirect.com

ORIGINAL ARTICLE

Corrosion resistance of electroless Cu–P and Cu–P–SiC composite coatings in 3.5% NaCl

Soheila Faraji [a], Afidah Abdul Rahim [a,*], Norita Mohamed [a], Coswald Stephen Sipaut [b], Bothi Raja [a]

[a] *School of Chemical Sciences, Universiti Sains Malaysia, 11800 USM, Penang, Malaysia*
[b] *School of Engineering and Information Technology, Universiti Malaysia Sabah, P.O. Box 2073, 88999 Kota Kinabalu, Sabah, Malaysia*

Received 26 August 2010; accepted 14 October 2010
Available online 20 October 2010

KEYWORDS

Electroless copper (EC);
SiC particles;
Corrosion;
Potentiodynamic polarisation;
Electrochemical impedance spectroscopy (EIS);
NaCl

Abstract The Cu–P and Cu–P–SiC composite coatings on carbon steel substrates were deposited via electroless plating. The anti-corrosion properties of Cu–P and Cu–P–SiC coatings were studied in 3.5% NaCl solution. The anti-corrosion properties of Cu–P and Cu–P–SiC coatings were investigated in 3.5% NaCl solution by the weight loss, potentiodynamic polarisation and electrochemical impedance spectroscopy (EIS) techniques. It has been found that the shift in the corrosion potential (E_{corr}) towards the noble direction, decrease in the corrosion current density (I_{corr}), increase in the charge transfer resistance (R_{ct}) and decrease in the double layer capacitance (C_{dl}) values indicated an improvement in corrosion resistance with the incorporation of SiC particles in the Cu–P matrix. The effects of varying the SiC concentration on the corrosion resistance of carbon steel were investigated and it was found that the best anti-corrosion property of Cu–P–SiC is at 5 g L^{-1} SiC in the bath formulation.

1. Introduction

Electroless plating is a technique to produce decorative plating layer of uniform deposition on complex shapes, conductive and non-conductive substrates using relatively simple equipment. At present, these plating layers are applied in many fields, such as in chemical, electronic and machinery industries (Mallory and Hadju, 1990). Electroless composite plating is a surface treatment technology developed on the basis of electroless plating. There is considerable interest in electrodeposited metallic alloys, since this process allows coatings to be obtained with better mechanical and physical properties, and a better corrosion resistance than layers made from individual

* Corresponding author. Tel.: +60 46533576.
E-mail address: afidah@usm.my (A.A. Rahim).

Peer-review under responsibility of King Saud University.
doi:10.1016/j.arabjc.2010.10.014

Production and hosting by Elsevier

metals (Balaraju and Rajam, 2005; Gan et al., 2008; Kanta et al., 2009).

Diversified metallic and nonmetallic surfaces endowed with attractive appearance, high corrosion resistance, electromagnetism, low density and some other special functions have been produced by electroless copper (EC). Thus this technique has been widely used in the electronic industry, aerospace industry and machinery manufacturing (Li, 2003). The extensive demand for these applications promotes the development of copper formulation and plating techniques. Conventional EC plating baths usually use formaldehyde (HCHO) as the reducing agent (Vaskelis et al., 2007). It is operated at pH values above 11 and this bath may release poisonous gases during operation. Recently glyoxylic acid (Wu and Sha, 2009) and hypophosphite (NaH_2PO_2) because of its low pH, low cost, and relative safety features (Cheng et al., 1997; Gan et al., 2007a,b, 2008) have been used to replace formaldehyde.

Carbon steel is one of the major construction materials used extensively in chemical and allied industries dealing with acidic, alkaline and salt solutions. The corrosion of carbon steel is a major infrastructure degradation problem in industries, including the chemical, mineral, materials and petrochemical industries world-wide (Noor and Al-Moubaraki, 2008). In order to improve the corrosion resistance of carbon steel, they are often alloyed or surface treated with more corrosion resistant metals such as Ni (Zhao and Liu, 2005), Zn (Barranco and Feliu, 2004), Sn (Sürme et al., 2009), Co (Bajat et al., 2002) and inhibitors (Laamari et al., 2010; Kamal et al., 2010). Because of its excellent corrosion-resistant properties, tin-plated carbon steel is frequently used for the production of beverage cans, food cans, and aerosol cans (Oni et al., 2008).

In recent years, electroless plating has won great popularity in preparing composite coatings, which are generally prepared by adding solid particles to the regular electroless plating solution to achieve co-deposition of the solid particles. The co-deposition improves the mechanical and tribological properties of coatings. The inclusion of ceramic particles such as: Al_2O_3 (Szczygiel and Kolodziej, 2005) and SiC (Zhang et al., 2008) into the metal matrix can significantly improve the hardness and anti-wear property of the matrix. Silicon carbide (SiC) can serve as both structured and functional materials for its good thermal conductivity, electrical conductivity, chemical stability, high mechanical strength, low friction and has high material strength with excellent corrosion, erosion resistance, mechanical and physical properties. SiC particles are of great technological importance for their applications as reinforcement of metal matrix composites and structural ceramics (Zhang et al., 2008; Li et al., 2006; Jiaqiang et al., 2006; Grosjean et al., 2001; Medeliene, 2002). In recent years, SiC has found new applications in the electronic industry for its excellent and adjustable dielectric properties (Zhao et al., 2008).

The SiC particles were successfully co-deposited in electroless Ni–P and were found to improve its corrosion resistance (Medeliene, 2002). However, the relatively cheaper cost of Cu materials, as compared to Ni, makes them more attractive for commercial applications in industries. It has also been reported that Cu–SiC composites have been used as a heat sink material for fusion applications owing to the high-thermal conductivity of Cu and the low swelling of SiC ceramic under neutron irradiation (Gan et al., 2008). Furthermore, copper and copper-based alloys are widely used in the electrical industry. The addition of ceramic reinforcements such as alumina, silicon carbide and cerium oxide to form metal matrix composites (MMCs) enhances the properties such as elastic modulus, higher strength, better wear resistance, higher coefficient of friction and high-temperature durability. These attractive properties are expected to widen the applications of copper composite materials compared to copper (Ramesh et al., 2009; Shu and Tu, 2001).

The aim of this work is to investigate the effects of incorporation of SiC particles and the SiC concentration on the anti-corrosion properties of Cu–P and Cu–P–SiC coatings on carbon steel substrates in 3.5% NaCl solution by using the weight loss, potentiodynamic polarisation and EIS techniques.

2. Experimental

2.1. Bath formulation

The pretreatment procedures as previously reported (Liu and Zhao, 2004) were used. The optimised solution compositions and the plating conditions for electroless Cu–P and Cu–P–SiC plating are given in Table 1. Steel sheets ($2.54 \times 2.54 \times 0.28$ cm, having a composition of C: 0.205%, Si: 0.06%, Mn: 0.55%, S: 0.047%, P: 0.039% and Fe% remaining) were first cleaned with 10% NaOH at 60–80 °C for 10–20 min (to remove grease) and then rinsed with water. They were dipped in 5% HCl solution for 30 s (pickling for the activation of the surface) (Jiaqiang et al., 2006) and then were rinsed with deionised water, before electroless Cu–P and Cu–P–SiC plating.

Sodium hypophosphite (as a reducing agent), sodium citrate (as a complexing agent), boric acid (as a buffering agent), nickel(II) sulfate (as a catalyst for hypophosphite oxidation) and polyglycol (as a surfactant) were used as received. SiC particles (4–10 μm in diameter) were added for SiC co-deposition and magnetic stirring was used to avoid sedimentation of particles.

2.2. Surface analysis

The coating surface morphology and the coating compositions were analysed and determined, respectively, using scanning electron microscopy (LEO SUPRA 55VP FESEM) equipped with an energy dispersive micro analysis system of Oxford INCA 400 X-ray (EDX) spectrometer. The X-ray diffraction patterns of Cu–P and Cu–P–SiC composite coatings were

Table 1 Composition (gL^{-1}) and operating conditions of electroless Cu–P and Cu–P–SiC coatings.

Components in bath	Cu–P	Cu–P–SiC
Copper sulfate (gL^{-1})	8	25
Sodium hypophosphite (gL^{-1})	60	125
Nickel sulfate (gL^{-1})	1	3.125
Sodium citrate (gL^{-1})	15.5	50
Boric acid (gL^{-1})	12.4	25
SiC (gL^{-1})	–	5
Polyglycol (gL^{-1})	0.001	0.001
Stabilizer (gL^{-1})	0.001	0.001
pH	9	9
T (°C)	75	90
Time (h)	3	1

analysed with a high resolution X-ray diffractometer system [PANalytical X'Pert PRO MRD PW3040].

2.3. Corrosion rate measurements

2.3.1. Weight loss technique

The Cu–P–SiC coating samples were polished with 230, 400, 600, 800, 1000 and 1200 grades of abrasive papers, washed thoroughly with distilled water, degreased with acetone and dried at room temperature (30 °C). The polished and pre-weighed Cu–P–SiC coating samples were immersed in 3.5% NaCl solution for 480 h (20 days) (Liu and Zhao, 2004; Zhao and Liu, 2005). Then the specimens were taken out, washed, dried and weighed. The procedure was repeated with Cu–P coatings and carbon steel substrates. The weight loss of Cu–P–SiC, Cu–P and carbon steel with immersion time t (hours) were expressed as mg cm^{-2}.

2.3.2. Potentiodynamic polarisation studies

Potentiodynamic polarisation studies were conducted by using PGP 201 potentiostat–galvanostat equipped with Volta Master 4 software for data acquisition. The electrolytes used were 3.5% NaCl solution in aerated conditions. The coated specimens were masked so that only 1 cm^2 area was exposed to the electrolyte. The working electrode (test samples) was polished using 230, 400, 600, 800, 1000 and 1200 grades of abrasive papers, washed with distilled water, degreased with acetone, thoroughly rinsed with distilled water and finally dried at room temperature (30 °C). A conventional glass cell was used. A luggin capillary was placed near the working electrode to minimise the solution resistance. A platinum foil was used as the counter electrode and the reference electrode was a saturated calomel electrode (SCE). During the potentiodynamic sweep experiments, the samples were first immersed into the electrolyte for 30 min to establish the open-circuit potential, E_0. Subsequently, potentiodynamic curves were recorded by sweeping the electrode potential from E_0 to 200 mV in both cathodic and anodic directions at a sweeping rate of 0.66 mV s^{-1}. Current and potential readings were recorded simultaneously. Tafel plots were obtained from the data and the corrosion current density (I_{corr}) was determined by extrapolating the straight-line section of the anodic and cathodic Tafel lines. The I_{corr} values were used to calculate the corrosion inhibition efficiency (IE%) of the coatings according to Eq. (1):

$$\mathrm{IE}(\%) = \left(1 - \frac{I_{corr(i)}}{I_{corr(0)}}\right) \times 100 \quad (1)$$

where $I_{corr(0)}$ and I_{corr} are the corrosion current densities for the carbon steel and the composite coatings, respectively.

2.3.3. Electrochemical impedance spectroscopy (EIS) studies

The electrochemical impedance spectroscopy (EIS) measurements were performed with Gamry Reference 600 (US). The employed amplitude of sinusoidal signal was 10 mV, and the frequency range was from 100 kHz to 10 mHz. The test electrolyte was 3.5% NaCl solution and the test temperature was maintained at 30 °C. The specimens that were embedded into an epoxy resin with an exposed area of 3.14 cm^2 were immersed in the solution for about 1 h before each test in order to establish the open circuit potential, E_0. The acquired data were curve fitted and analysed using Gamry Echem Analyst software. Both Nyquist and Bode plots were used to describe the corrosion behavior of electroless Cu–P and Cu–P–SiC composite coatings. The impedance values ($|Z|$) of the coatings were calculated from the Bode impedance plots. The Bode phase angle plots were also analysed to understand the mechanism of corrosion of the Cu–P and Cu–P–SiC composite coatings and carbon steel substrates.

3. Results and discussion

3.1. Surface analysis

The SEM micrographs of the coatings from the optimal bath conditions are shown in Fig. 1. Fig. 1b shows the presence of the SiC particles on the Cu–P–SiC coating. Fig. 2 shows the element compositions (wt.%) of electroless Cu–P and Cu–P–SiC coatings measured using EDX. The Cu content on the composite coatings surface was above 75%. The deposition of Cu–P and Cu–P–SiC coatings is also supported by the XRD results. The XRD of the Cu–P coating showed the presence of Cu_2O and Cu_3P while the Cu–P–SiC coating depicted the presence of Cu_2O, Cu_3P, Cu_3Si and SiC (Fig. 3).

3.2. Corrosion rate measurements

3.2.1. Weight loss technique

The anti-corrosion performance of the Cu–P–SiC coatings in 3.5% NaCl solution was compared with that of Cu–P coatings

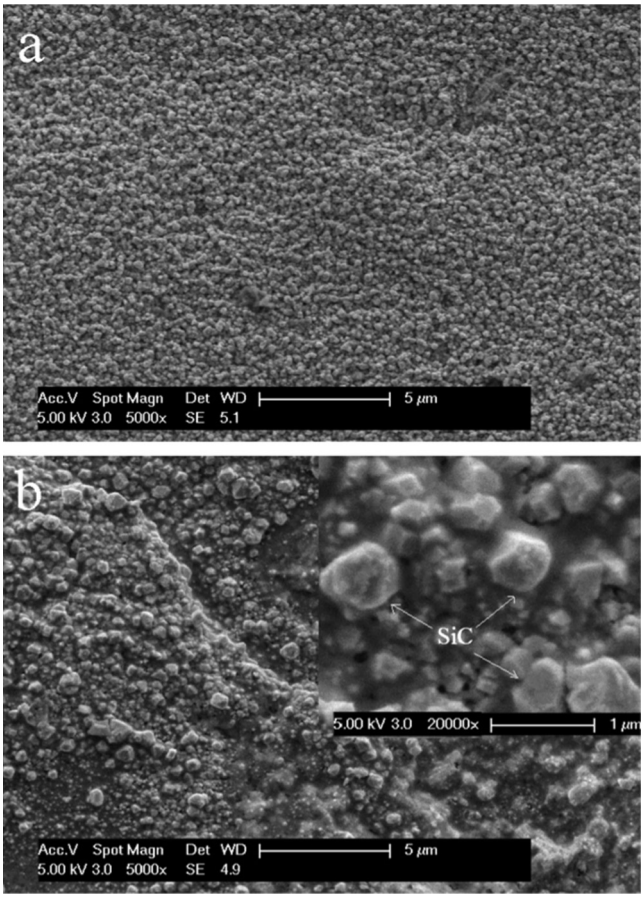

Figure 1 SEM of (a) Cu–P, (b) Cu–P–SiC composite coatings.

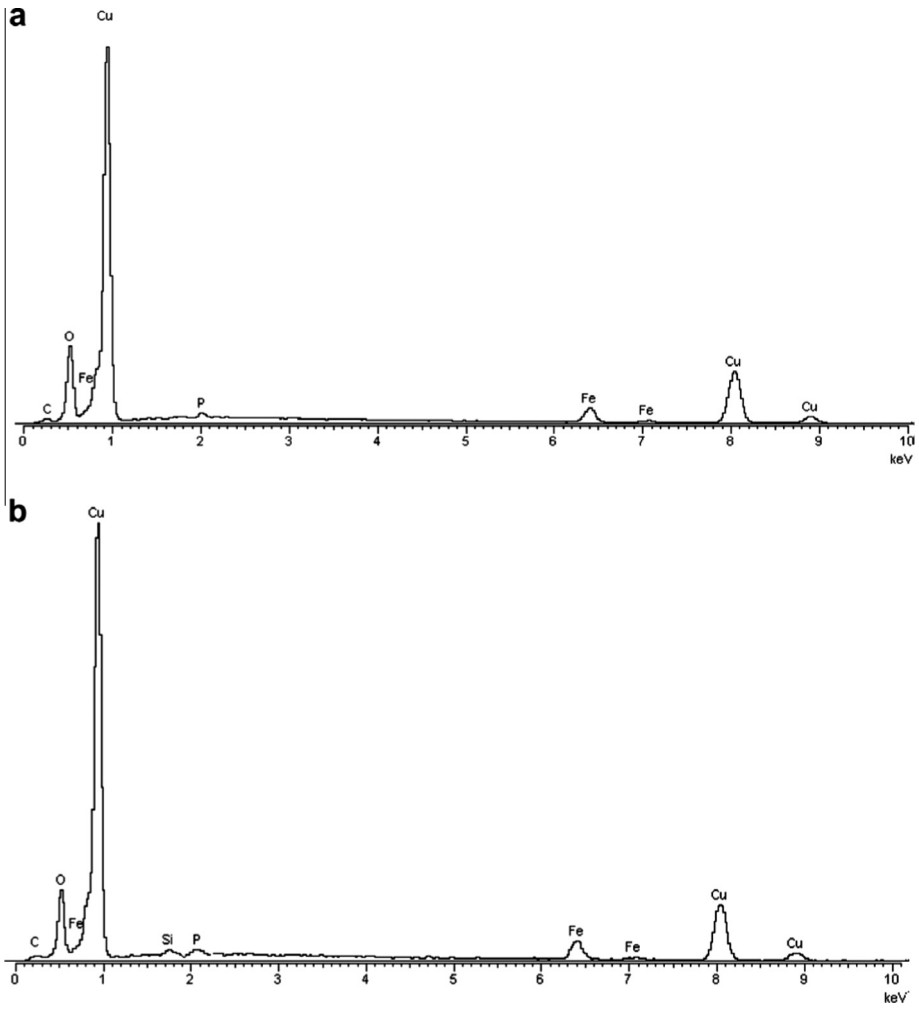

Figure 2 EDX of the surface of the composites: (a) Cu–P, (b) Cu–P–SiC.

and carbon steel substrates via the weight loss method (Fig. 4). Fig. 4 shows the comparison of the corrosion rates of carbon steel substrates, Cu–P and Cu–P–SiC composite coatings in 3.5% NaCl solution during the 480 h (20 days) corrosion tests. For the carbon steel substrate an almost linear increase of weight loss with respect to time was observed. On the other hand, a minimum increase in weight loss for the Cu–P and Cu–P–SiC coatings was observed only after 200 h of immersion. These curves also show that after 480 h immersion in 3.5% NaCl solution, carbon steel has the highest weight loss of 4.49 mg cm^{-2} and Cu–P–SiC the lowest weight loss of 3.25 mg cm^{-2} in 3.5% NaCl solution. Thus incorporation of SiC into the coatings improved the corrosion-resistant properties of the coatings. Fig. 5 shows that the corrosion rate of the coatings decreased from 4 to 5 g L^{-1} and then increased at 6 g L^{-1}. This could be explained by the fact that when the concentration of SiC particles in the bath increases, the deposition of SiC particles on the coating surface accelerates accordingly due to the agitating action of solution (Zhang et al., 2008). However, the congregation among particles in solution tends to start when the particle content increases to a certain degree. In other words, suspension and congregation in solution increase with increasing SiC concentration. Consequently, the coating would be rough and uneven. The increase in weight of congregated SiC particles prevents them from floating (Zhang et al., 2008). Hence, the effective SiC concentration decreases and the deposition rate and Cu content in the coating will decrease slowly. So the Cu–P–SiC coatings at 5 g L^{-1} SiC have the lowest weight loss for the bath that is given in Table 1.

3.2.2. Potentiodynamic polarisation studies

The electrochemical results obtained from the polarisation studies for the electroless carbon steel, Cu–P and Cu–P–SiC coatings in aerated 3.5% sodium chloride are shown in Table 2 and Fig. 6. The electrochemical corrosion parameters obtained from the Tafel polarisation curves are given in Table 2.

In general, the corrosion resistance of any alloy depends on the rate of formation of a surface protective film; in this case, Cu_2O, Cu_3P, Cu_3Si and SiC as confirmed by XRD. The Cu–P and Cu–P–SiC coatings show relatively good resistance to corrosion in 3.5% NaCl as witnessed from Fig. 6. The presence of phosphorus and silicon carbide shifted the corrosion potential, E_{corr}, to the right and decreased the corrosion current density, I_{corr} and consequently improved the corrosion resistance. Comparison of the electrochemical parameters (Table 2) of the electroless Cu–P, Cu–P–SiC composite coatings and carbon steel reveal that E_{corr} shifted towards the more noble direction, I_{corr} values decreased and R_p increased with the

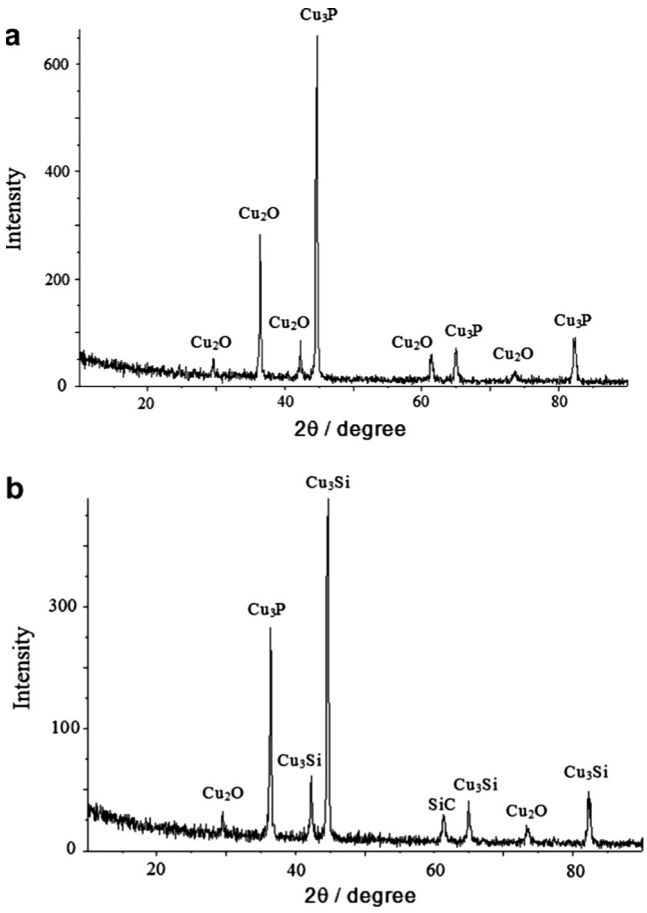

Figure 3 X-ray diffraction patterns of the (a) Cu–P, (b) Cu–P–SiC coatings.

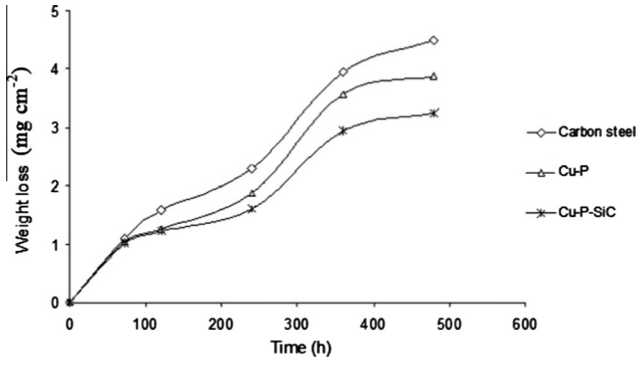

Figure 4 Comparison of Cu–P–SiC with Cu–P and carbon steel in inhibition of 3.5% NaCl corrosion.

incorporation of SiC particles in the electroless matrix, indicating a better corrosion protective ability of coatings. (Krishnaveni et al., 2009)

Fig. 7 illustrates the polarisation curves of the Cu–P–SiC coatings with different SiC concentrations in the 3.5% NaCl solutions. It can be seen, I_{corr} and annual corrosion rate of the coatings decreased from 4 until 5 g L^{-1} and then increased at 6 g L^{-1} as similarly observed from the weight loss measurement for the same reasons as explained in the section on the

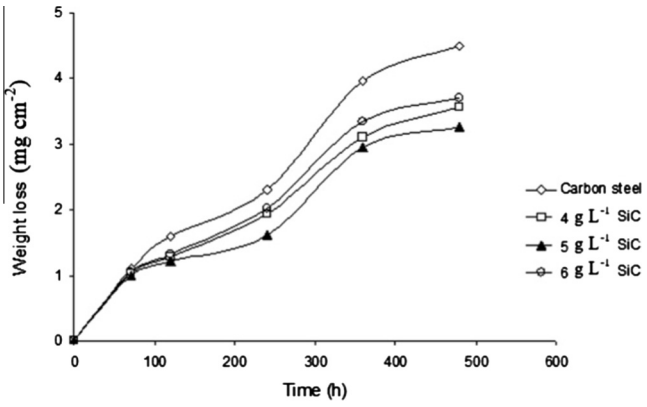

Figure 5 Comparison of Cu–P–SiC coatings with different concentrations of SiC and carbon steel in inhibition of 3.5% NaCl corrosion.

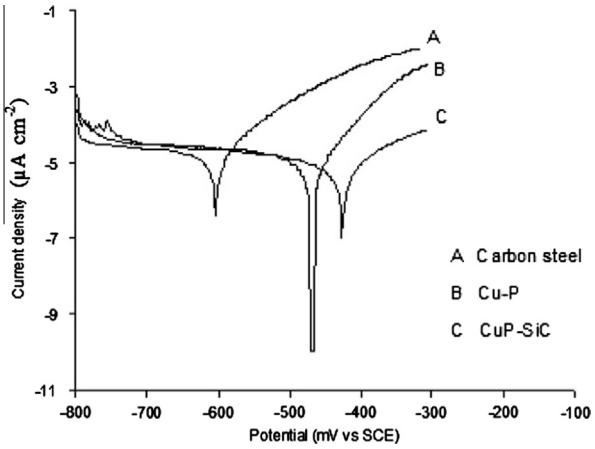

Figure 6 Potentiodynamic polarisation curves of as plated electroless Cu–P, Cu–P–SiC coatings and carbon steel in 3.5% NaCl solution.

weight loss technique. So the Cu–P–SiC coatings at 5 g L^{-1} SiC has the highest R_p, the lowest I_{corr} and the lowest annual corrosion rate.

The order of increasing corrosion resistance is as follows: carbon steel < Cu–P < Cu–P–SiC. The corrosion rate was reduced to a third of its value while the corrosion inhibition efficiency (IE%) of Cu–P–SiC coatings reached 65% with the incorporation of P and SiC in the matrix for Cu–P–SiC coatings for the bath that contained 5 g L^{-1} SiC (Table 2).

3.2.3. Electrochemical impedance spectroscopy (EIS) studies

The measured impedance spectra of the carbon steel substrate, electroless Cu–P and Cu–P–SiC composite coatings in 3.5% NaCl solution are shown as Nyquist plots in Fig. 8, Bode and Bode phase plots in Figs. 9 and 10, respectively. It is evident from Fig. 8 that the substrate exhibits a semicircle in the high frequency region followed by a loop in the low frequency region which corresponds to the decrease of impedance $|Z|$ at the low frequency in the Bode plot as compared to Cu–P and Cu–P–SiC coatings (Fig. 9). The formation of a single semicircle or a semicircle in the high frequency region followed

Table 2 Corrosion characteristics of as plated electroless Cu–P, Cu–P–SiC coatings and carbon steel in 3.5% NaCl solution by potentiodynamic polarisation.

Specimens SiC (g L^{-1})	E_{corr} (mV vs SCE)	R_p (KΩ cm^2)	I_{corr} (μA cm^{-2})	Corrosion rate (mm $year^{-1}$)	IE%
Cu–P–SiC 4	−486.7	3.01	4.98	58.01	54.5
Cu–P–SiC 5	−429.8	3.68	3.77	43.76	65.6
Cu–P–SiC 6	−479.3	3.45	4.11	49.20	62.5
Cu–P	−472.6	2.68	6.53	75.80	40.4
Carbon steel	−607.4	1.55	10.96	130.00	0.0

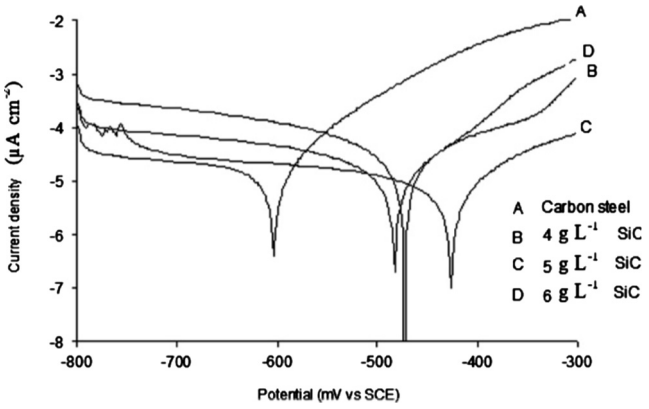

Figure 7 Potentiodynamic polarisation curves of as plated electroless Cu–P–SiC coatings with different concentrations of SiC and carbon steel in 3.5% NaCl solution.

by a low frequency loop is typical of metallic coatings (Li et al., 2009). Although the curves in the Nyquist plot appear to be similar with respect to their shape, they differ considerably in their sizes. This indicates that the same fundamental processes must be occurring on both the Cu–P and Cu–P–SiC composite coatings but over a different effective area in each case. The semicircle at the high frequency region represents the coating response, while the loop at the low frequency region is associated with simultaneous physicochemical phenomena at the metal/coating/solution interface (Krishnaveni et al., 2009; Li et al., 2009). According to Contreras et al. (2006) and Krishnaveni et al. (2009) the loop at the lower frequency region is associated with the double layer capacitance and/or diffusion phenomena of the oxidant chemical species through the porous coating.

In order to have a better insight on the coating response as well as the diffusion phenomenon, Bode impedance (Fig. 9) and Bode phase angle plots (Fig. 10) were constructed. The

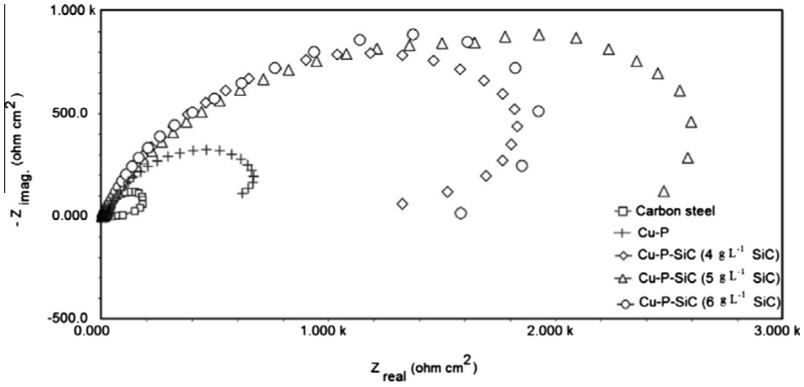

Figure 8 Nyquist plots of electroless Cu–P, Cu–P–SiC coatings and carbon steel in 3.5% NaCl solutions.

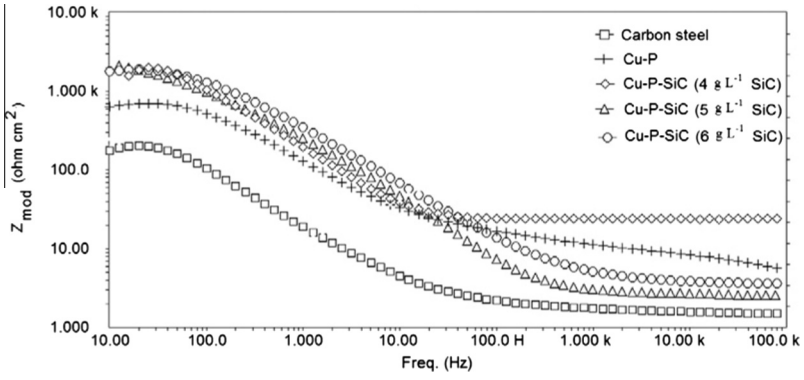

Figure 9 Bode plots of electroless Cu–P, Cu–P–SiC coatings and carbon steel in 3.5% NaCl solutions.

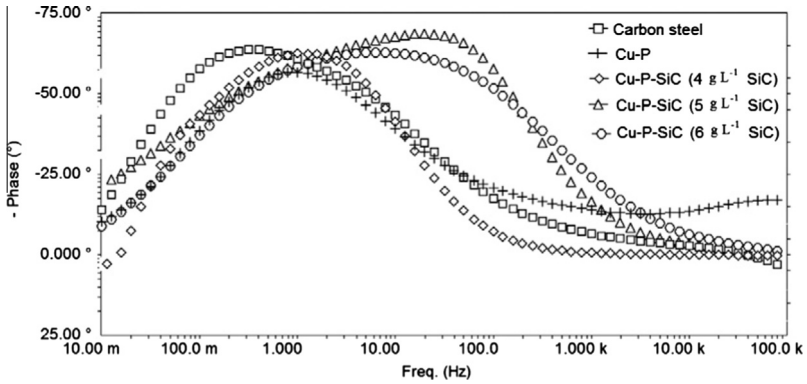

Figure 10 Bode phase plots of electroless Cu–P, Cu–P–SiC coatings and carbon steel in 3.5% NaCl solutions.

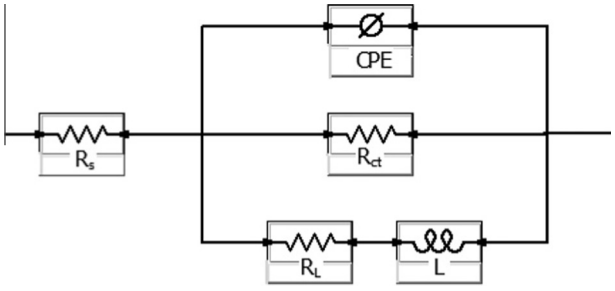

Figure 11 Electrochemical equivalent circuits used for fitting the experimental data of electroless Cu–P, Cu–P–SiC coatings and carbon steel, R_s: solution resistance; CPE: constant phase element; R_{ct}: charge-transfer resistance; R_L: inductance resistance; L: inductance.

Table 3 Corrosion characteristics of as plated electroless Cu–P–SiC, Cu–P coatings and carbon steel substrate in 3.5% NaCl solution obtained from electrochemical impedance (EIS) studies.

Specimens SiC (g L^{-1})	R_{ct} (Ω cm^2)	C_{dl} (μF cm^{-2})
Cu–P–SiC 4	2105.00	1.52
Cu–P–SiC 5	2440.00	1.48
Cu–P–SiC 6	2352.00	1.50
Cu–P	1054.00	9.86
Carbon steel	98.33	41.7

composite coatings offer relatively better corrosion resistance than carbon steel substrate that leads to an increase in their corrosion protective ability. The Bode phase angle plots of the electroless Cu–P, Cu–P–SiC composite coating and carbon steel suggested the involvement of one time constant characteristic of active corrosion and thus it is concluded that only one mechanism prevailed for the corrosion coatings and that the occurrence could be related to the electrolyte/coating interface. (Krishnaveni et al., 2009; Li et al., 2009; Contreras et al., 2006; Ma et al., 2006)

The equivalent circuit (Fig. 11) was used for fitting the EIS data of the carbon steel substrate and the coatings. The circuit as shown in Fig. 11 consists of the solution resistance (R_s), inductance resistance (R_L), inductance (L), charge transfer resistance (R_{ct}) and a constant phase element (CPE), which replaces the capacitance of the double layer (C_{dl}) due to the roughness and inhomogeneity of the electrode surface (Li et al., 2009, 2007; Ma et al.,2006). To obtain C_{dl}, the frequency (f_{max}) at which the imaginary component of the impedance is maximal was found and used in Eq. (2):

$$C_{dl} = (2\pi f_{max} R_{ct})^{-1} \quad (2)$$

The R_{ct} and C_{dl} values of the electroless Cu–P and Cu–P–SiC composite coatings are compiled in Table 3. It has been established that high values of R_{ct} and low values of C_{dl} imply a better corrosion protective ability of coatings (Krishnaveni et al., 2009; Li et al., 2009; Lin and Duh, 2009), while the C_{dl} value is also related to the porosity of the coating

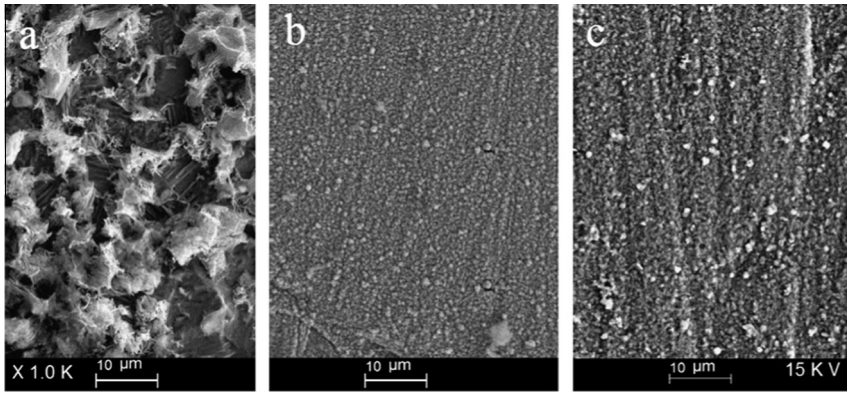

Figure 12 SEM of the surface of (a) carbon steel substrate, (b) Cu–P and (c) Cu–P–SiC composite coatings after corrosion processes in 3.5% NaCl.

(Krishnaveni et al., 2009; Contreras et al., 2006; Lin and Duh, 2009). The R_{ct} and C_{dl} values increased and decreased, respectively, with the incorporation of SiC in the Cu–P composite coatings. The Cu–P–SiC with 5 g L^{-1} SiC has the highest values of R_{ct} and lowest values of C_{dl} implying the better anti-corrosion ability. The R_{ct} of Cu–P–SiC with 5 g L^{-1} SiC and Cu–P composite coatings are 2440 and 1054 $\Omega\,cm^2$, respectively, and the corresponding C_{dl} values are 1.48 and 9.86 $\mu F\,cm^{-2}$, respectively.

The improvement of the corrosion resistance of the electroless composite coatings depends on the chemical stability of the particles, effective metallic area prone to corrosion, structural state of the coating, porosity or defect size of the coating, ability to prevent diffusion of chloride ions along the interface between the metal and the particle, the ability of the particle to prevent the corrosive pits from growing up, etc. (Krishnaveni et al., 2009). It is suggested that the SiC particles are chemically stable in 3.5% NaCl and the incorporation of SiC particles in the Cu–P matrix would decrease the effective metallic area prone to corrosion. The occurrence of a loop in the low frequency region in the Nyquist plot and the Bode plot confirms the penetration of the chloride ions and creation of the electrolyte-substrate interface in the substrate. An improvement of the corrosion resistance of Cu–P–SiC composite coatings compared to Cu–P was also observed in this study. This could be due to the fact that the SiC particles in this study are capable of filling some of the pores in the coating and prevent further diffusion of chloride ions along the interface. From the Nyquist plot (Fig. 8) it also can be seen that the Cu–P–SiC with 5 g L^{-1} SiC in the bath formulation exhibits the biggest semicircle radius compared to the other Cu–P–SiC, Cu–P composite coatings and carbon steel substrate and is expected to exhibit the best corrosion resistance, consistent with the potentiodynamic polarisation and weight loss results.

The improvement in corrosion resistance observed for the Cu–P–SiC composite coatings compared to the Cu–P coating could have resulted from the decrease in effective metallic area prone to corrosion. Otherwise, the enhancement of the anti-corrosion property may be attributed to the following reasons as proposed by Li et al. on Ni–TiO_2 composite coating (Li et al., 2009). In this study, the SiC particles embedded in the metal Cu matrix act as physical barriers to the initiation and development of corrosion defects, hence the microstructure of the copper layer is modified and the corrosion resistance of the coating is improved. In addition, the co-deposition of the SiC particles in the composite coating can help to

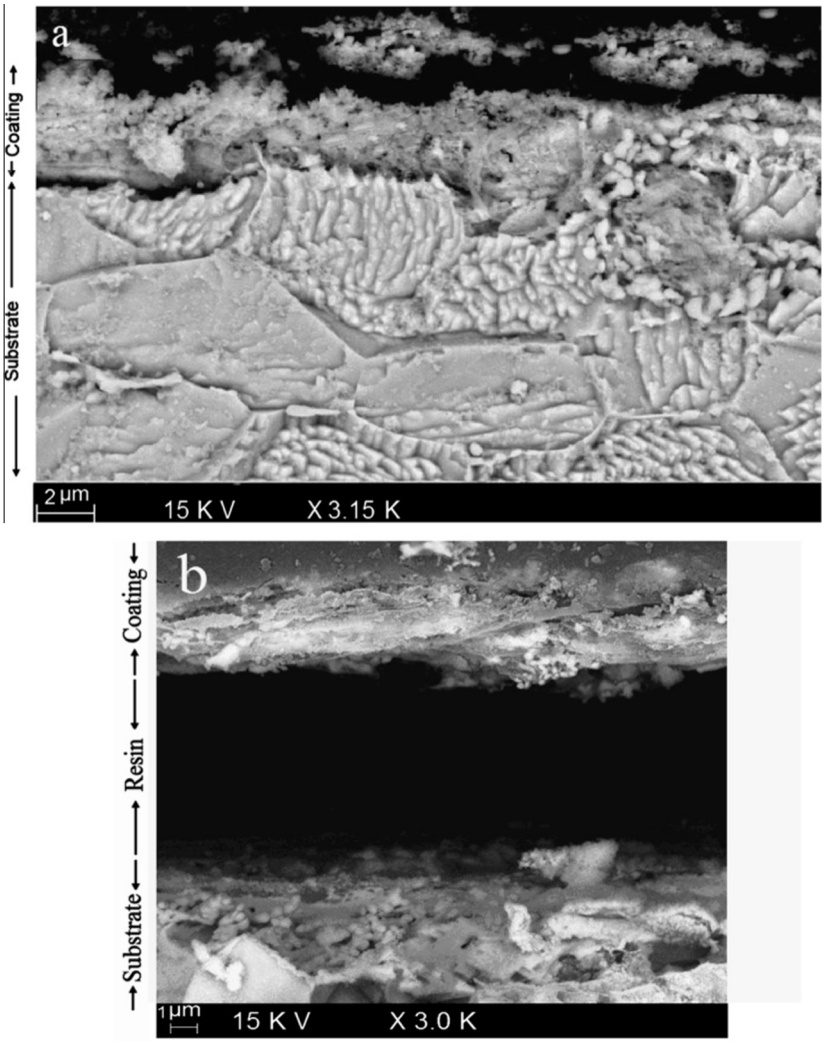

Figure 13 SEM image of the cross section of the Cu–P–SiC coating (a) after and (b) before corrosion processes in 3.5% NaCl.

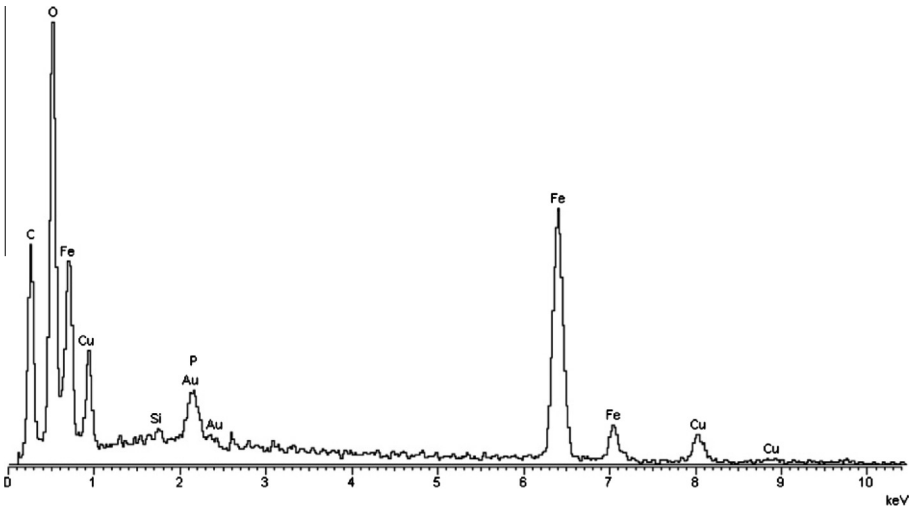

Figure 14 EDX of the cross section of the Cu–P–SiC coating after corrosion processes in 3.5% NaCl.

accelerate the passivation process of the metal substrate. Consequently, the corrosion resistance of the carbon steel coated with the SiC composite coating was improved. The EIS results also confirm that the Cu–P–SiC composite coating elevates the anti-corrosion performance of specimens remarkably consistent with the results of the potentiodynamic polarisation technique and weight loss test.

3.3. Morphology of cross-sections of electroless Cu–P–SiC coatings

Fig. 12 shows the SEM images of the substrate and coatings. A transformation of morphology was observed. The smoother surface shown by the coatings indicated the protective behavior of the coatings against corrosion.

SEM images of the cross-sections of the electroless Cu–P–SiC coatings before and after immersion in NaCl solutions from the polarisation measurements were taken. The Cu–P–SiC composite coating before immersion in the NaCl solution showed that the incorporated particles are evenly distributed in the composite matrix and are firmly bonded to the substrate with copper content of 74 wt.%. The micrographs of the Cu–P–SiC coating upon immersion in 3.5% NaCl showed that the composite matrix was less compact and loosely bonded to the substrate (Fig. 13a) compared to the coatings before the corrosion process (Fig. 13b), allowing easy access of the Cl^- ions to penetrate the coating and interact with the carbon steel substrate. It is interesting to note that only Cu was removed while the P and SiC contents remained almost unchanged after the corrosion process as shown from the EDX results of the Cu–P–SiC coating; before (Fig. 2b) and after (Fig. 14) corrosion processes. The EDX results showed that the copper content has been reduced to 22.5%. The decreased corrosion rate that was obtained from the weight loss and potentiodynamic polarisation techniques seem to indicate that the corrosion resistance is related to the reduction of the Cu content in the coating.

4. Conclusion

In summary, the following conclusions have been drawn from the present investigation.

(1) The weight loss, potentiodynamic polarisation and EIS techniques showed that, the anti-corrosion performance of these Cu–P–SiC composite coatings was superior to that of the Cu–P coatings and carbon steel substrates.
(2) The incorporation of SiC particles in the Cu–P matrix shifted the E_{corr} towards the noble direction, decreased I_{corr} and C_{dl} and increased R_p and R_{ct} values.
(3) The best anti-corrosion property of Cu–P–SiC is at 5 g L^{-1} SiC in the bath formulation for carbon steel substrates.

Acknowledgments

The authors acknowledge Universiti Sains Malaysia for the financial support of this research under the Research Universiti Sains Grant (RU. Grant No: 1001/PKIMIA/811006). The authors also would like to thank the Universite Henri Poincare (France) for the use of their SEM facilities.

References

Bajat, J.B., Miskovic-Stankovic, V.B., Kacarevic-Popovic, Z., 2002. Electrochemical and sorption characteristics and thermal stability of epoxy coatings electrodeposited on steel modified by Zn–Co alloy. Prog. Org. Coat. 45, 379–387.

Balaraju, J.N., Rajam, K.S., 2005. Electroless deposition of Ni–Cu–P, Ni–W–P, Ni–W–Cu–P alloys. Surf. Coat. Technol. 201, 154–161.

Barranco, V., Feliu, S., 2004. EIS study of the corrosion behaviour of zinc-based coatings on steel in quiescent 3% NaCl solution. Part 1: Directly exposed coatings. Corr. Sci. 46, 2203–2220.

Cheng, D.H., Xu, W.Y., Zhang, Z.Y., Yiao, Z.H., 1997. Electroless copper plating using hypophosphite as reducing agent. Met. Finish. 95, 34–37.

Contreras, A., León, C., Jimenez, O., Sosa, E., Pérez, R., 2006. Electrochemical behavior and microstructural characterization of 1026 Ni–B coated steel. Appl. Surf. Sci. 253, 592–599.

Gan, X., Wu, Y., Liu, L., Shen, B., Hu, W., 2007a. Electroless copper plating on PET fabrics using hypophosphite as reducing agent. Surf. Coat. Technol. 201, 7018–7023.

Gan, X., Wu, Y., Liu, L., Hu, W., 2007b. Effects of $K_4Fe(CN)_6$ on electroless copper plating using hypophosphite as reducing agent. J. Appl. Electrochem. 37, 899–904.

Gan, K., Gu, M., Mu, G., 2008. Effect of Fe on the properties of Cu/SiC_p composite. J. Mater. Sci. 43, 1318–1323.

Gan, X., Wu, Y., Liu, L., Shen, B., Hu, W., 2008. Electroless plating of Cu–Ni–P alloy on PET fabrics and effect of plating parameters on the properties of conductive fabrics. J. Alloys Compd. 455, 308–313.

Grosjean, A., Rezrazi, M., Takadoum, J., Berçot, P., 2001. Hardness, friction and wear characteristics of nickel–SiC electroless composite deposits. Surf. Coat. Technol. 137, 92–96.

Jiaqiang, G., Lei, L., Yating, W., Bin, S., Wenbin, H., 2006. Electroless Ni–P–SiC composite coatings with superfine particles. Surf. Coat. Technol. 200, 5836–5842.

Kamal, C., Sethuraman, M.G., 2010. Spirulina platensis – a novel green inhibitor for acid corrosion of mild steel. Arab. J. Chem.. doi:10.1016/j.arabjc.2010.08.006.

Kanta, A.F., Vitry, V., Delaunois, F., 2009. Wear and corrosion resistance behaviours of autocatalytic electroless plating. J Alloys Compd. 486, L21–L23.

Krishnaveni, K., Narayanan, T.S.N.S., Seshadri, S.K., 2009. Corrosion resistance of electrodeposited Ni–B and Ni–B–Si_3N_4 composite coatings. J. Alloys Compd. 480, 765–770.

Laamari, R., Benzakour, J., Berrekhis, F., Abouelfida, A., Derja, A., Villemin, D., 2010. Corrosion inhibition of carbon steel in hydrochloric acid 0.5 M by hexa methylene diamine tetramethylphosphonic acid. Arab. J. Chem.. doi:10.1016/j.arabjc.2010.06.046.

Li, N., 2003. Applied Technology of Electroless Plating. Chemical Engineering Publisher, Beijing.

Li, L., An, M., Wu, G., 2006. A new electroless nickel deposition technique to metallise SiC_p/Al composites. Surf. Coat. Technol. 200, 5102–5112.

Li, M., Jiang, L., Zhang, W., Qian, Y., Luo, S., Shen, J., 2007. Electrochemical corrosion behavior of nanocrystalline zinc coatings in 3.5% NaCl solutions. J. Solid State Electrochem. 11, 1319–1325.

Li, Q., Yang, X., Zhang, L., Wang, J., Chen, B., 2009. Corrosion resistance and mechanical properties of pulse electrodeposited Ni–TiO_2 composite coating for sintered NdFeB magnet. J. Alloys Compd. 482, 339–344.

Lin, C.H., Duh, J.G., 2009. Electrochemical impedance spectroscopy (EIS) study on corrosion performance of CrAlSiN coated steels in 3.5 wt.% NaCl solution. Surf. Coat. Technol. 204, 784–787.

Liu, Y., Zhao, Q., 2004. Study of electroless Ni–Cu–P coatings and their anti-corrosion properties. Appl. Surf. Sci. 228, 57–62.

Ma, C.B., Cao, F.H., Zhang, Z., Zhang, J.Q., 2006. Electrodeposition of amorphous Ni–P coatings onto Nd–Fe–B permanent magnet substrates. Appl. Surf. Sci. 253, 2251–2256.

Mallory, G.O., Hadju, J.B., 1990. Electroless Plating – Fundamentals & Applications. Noyes Publications, New York.

Medeliene, V., 2002. The influence of B_4C and SiC additions on the morphological, physical, chemical and corrosion properties of Ni coatings. Surf. Coat. Technol. 154, 104–111.

Noor, E.A., Al-Moubaraki, A.H., 2008. Corrosion behavior of mild Steel in hydrochloric acid solutions. Int. J. Electrochem. Sci. 3, 806–818.

Oni, B.O., Egieborb, N.O., Ekekwea, N.J., Chuku, A., 2008. Corrosion behavior of tin-plated carbon steel and aluminum in NaCl solutions using electrochemical impedance spectroscopy. J. Miner. Mater. Character. Eng. 7, 331–346.

Ramesh, C.S., Noor Ahmed, R., Mujeebu, M.A., Abdullah, M.Z., 2009. Development and performance analysis of novel cast copper–SiC–Gr hybrid composites. Mater. Des. 30, 1957–1965.

Shu, K.M., Tu, G.C., 2001. Fabrication and charachterization of Cu–SiC_p composites for electrical discharge machining application. Mater. Manufactur. Process 16, 483–502.

Sürme, Y., Gürten, A.A., Bayol, E., Ersoy, E., 2009. Systematic corrosion investigation of various Cu–Sn alloys electrodeposited on mild steel in acidic solution: dependence of alloy composition. J. Alloys Compd. 485, 98–103.

Szczygiel, B., Kolodziej, M., 2005. Composite Ni/Al_2O_3 coatings and their corrosion resistance. Electrochim. Acta 50, 4188–4195.

Vaskelis, A., Jaciauskiene, J., Stalnioniene, I., Norkus, E., 2007. Accelerating effect of ammonia on electroless copper deposition in alkaline formaldehyde-containing solutions. J. Electroanal. Chem. 600, 6–12.

Wu, X., Sha, W., 2009. Experimental study of the voids in the electroless copper deposits and the direct measurement of the void fraction based on the scanning electron microscopy images. Appl. Surf. Sci. 255, 4259–4266.

Zhang, S., Han, K., Cheng, L., 2008. The effect of SiC particles added in electroless Ni–P plating solution on the properties of composite coatings. Surf. Coat. Technol. 202, 2807–2812.

Zhao, Q., Liu, Y., 2005. Comparisons of corrosion rates of Ni–P based composite coatings in HCl and NaCl solutions. Corr. Sci. 47, 2807–2815.

Zhao, H.F., Tang, W.Z., Li, C.M., Chen, G.C., Lu, F.X., Cai, Y.H., Guo, H., Zhang, R.Q., Zhang, P.W., 2008. Thermal conductive properties of Ni–P electroless plated SiC_p/Al composite electronic packaging material. Surf. Coat. Technol. 202, 2540–2544.